

## Secondary aerosol formation and oxidation capacity in photooxidation in the presence of Al<sub>2</sub>O<sub>3</sub> seed particles and SO<sub>2</sub>

Biwu Chu<sup>1</sup>, Tengyu Liu<sup>2</sup>, Xiao Zhang<sup>3,4</sup>, Yongchun Liu<sup>1</sup>, Qingxin Ma<sup>1</sup>, Jinzhu Ma<sup>1</sup>, Hong He<sup>1\*</sup>,  
Xinming Wang<sup>2</sup>, Junhua Li<sup>3</sup> & Jiming Hao<sup>3</sup>

<sup>1</sup>State Key Joint Laboratory of Environment Simulation and Pollution Control; Research Center for Eco-Environmental Sciences, Chinese Academy of Sciences, Beijing 100085, China

<sup>2</sup>State Key Laboratory of Organic Geochemistry; Guangzhou Institute of Geochemistry, Chinese Academy of Sciences, Guangzhou 510640, China

<sup>3</sup>State Key Joint Laboratory of Environment Simulation and Pollution Control; School of Environment, Tsinghua University, Beijing 100084, China

<sup>4</sup>Nanjing University of Information Science & Technology, Nanjing 210044, China

Received March 11, 2015; accepted April 30, 2015; published online July 1, 2015

To investigate the sensitivity of secondary aerosol formation and oxidation capacity to NO<sub>x</sub> in homogeneous and heterogeneous reactions, a series of irradiated toluene/NO<sub>x</sub>/air and α-pinene/NO<sub>x</sub>/air experiments were conducted in smog chambers in the absence or presence of Al<sub>2</sub>O<sub>3</sub> seed particles. Various concentrations of NO<sub>x</sub> and volatile organic compounds (VOCs) were designed to simulate secondary aerosol formation under different scenarios for NO<sub>x</sub>. Under “VOC-limited” conditions, the increasing NO<sub>x</sub> concentration suppressed secondary aerosol formation, while the increasing toluene concentration not only contributed to the increase in secondary aerosol formation, but also led to the elevated oxidation degree for the organic aerosol. Sulfate formation was suppressed with the increasing NO<sub>x</sub> due to a decreased oxidation capacity of the photooxidation system. Secondary organic aerosol (SOA) formation also decreased with the presence of high concentration of NO<sub>x</sub>, because organo-peroxy radicals (RO<sub>2</sub>) react with NO<sub>x</sub> instead of with peroxy radicals (RO<sub>2</sub> or HO<sub>2</sub>), resulting in the formation of volatile organic products. The increasing concentration of NO<sub>x</sub> enhanced the formation of sulfate, nitrate and SOA under “NO<sub>x</sub>-limited” conditions, in which the heterogeneous reactions played an important role. In the presence of Al<sub>2</sub>O<sub>3</sub> seed particles, a synergetic promoting effect of mineral dust and NO<sub>x</sub> on secondary aerosol formation in heterogeneous reactions was observed in the photooxidation. This synergetic effect strengthened the positive relationship between NO<sub>x</sub> and secondary aerosol formation under “NO<sub>x</sub>-limited” conditions but weakened or even overturned the negative relationship between NO<sub>x</sub> and secondary aerosol formation under “VOC-limited” conditions. Sensitivity of secondary aerosol formation to NO<sub>x</sub> seemed different in homogeneous and heterogeneous reactions, and should be both taken into account in the sensitivity study. The sensitivity of secondary aerosol formation to NO<sub>x</sub> was further investigated under “winter-like” and NH<sub>3</sub>-rich conditions. No obvious difference for the sensitivity of secondary aerosol formation except nitrate to NO<sub>x</sub> was observed.

**secondary aerosol, oxidation capacity, synergetic promoting effect, Al<sub>2</sub>O<sub>3</sub> seed particles, sensitivity**

\*Corresponding author (email: honghe@rcees.ac.cn)

## 1 Introduction

In recent years, haze has increased in frequency of occurrence in eastern China as well as the area affected [1]. Particulate matter (PM), especially fine particulate matter (PM<sub>2.5</sub>), is the main cause of the haze. PM<sub>2.5</sub> is mainly contributed by secondary aerosol formation during atmospheric homogeneous and heterogeneous reactions. Sulfate, nitrate, and ammonia (SNA), contribute to 40%–60% of PM<sub>2.5</sub> mass [2,3]. Meanwhile, more than half of the organic mass in PM<sub>2.5</sub> is also generated by atmospheric reactions rather than being directly emitted from pollution sources [4–6]. Therefore, over 60% of PM<sub>2.5</sub> mass is secondary species. Higher ratio and “explosive growth” of secondary species in PM<sub>2.5</sub> were observed during heavy haze pollution [7]. Compared with London smog event [8], the SO<sub>2</sub> concentration in eastern China is much lower, but the PM pollution levels of haze are close, indicating a decrease of environmental capacity in eastern China [1].

It is well known that the emissions of oxides of nitrogen (NO<sub>x</sub>, NO+NO<sub>2</sub>), volatile organic compounds (VOCs), sulfur compounds (mainly SO<sub>2</sub>) and ammonia gas (NH<sub>3</sub>) lead to complex chemical and physical transformations and result in the formation of ozone (O<sub>3</sub>) and secondary aerosol. The production of sulfate and nitrate depends on the concentration of the precursors as well as the levels of oxidants (or oxidation capacity) [9]. The characteristics of preexisting seed particles [10–14], and meteorological conditions [10,15] were also found to play important roles in secondary aerosol formation, resulting in a highly non-linear relationship between PM formation and precursors [16,17]. It is important to understand how these factors individually and collectively affect the production of secondary aerosols under different conditions [9]. The non-linear relationship [18] between tropospheric O<sub>3</sub> production and concentrations of VOCs and NO<sub>x</sub> was well summarized by Seinfeld and Pandis [19]. In the O<sub>3</sub> isopleth diagram, with the decreasing NO<sub>x</sub> concentration, O<sub>3</sub> concentration decreased in the “NO<sub>x</sub>-limited” region, but increased in the “VOC-limited” region. “NO<sub>x</sub>-limited” or “VOC-limited” could be distinguished according to the ratio of VOC/NO<sub>x</sub>, which varies from location to location [19].

Secondary aerosol formation is closely related to the oxidation capacity, and therefore, affected by the ratio of VOC/NO<sub>x</sub>. Secondary organic aerosol (SOA), which is a major species in atmospheric particles and a research hotspot in atmospheric chemistry [20,21], was usually found to have lower yield with lower ratios of VOC/NO<sub>x</sub> [22,23]. In the atmosphere, SNA and SOA generation are not separated, but few studies have investigated their interaction [24]. The effects of the oxidation of SO<sub>2</sub> on the photooxidation of VOCs and NO<sub>x</sub> and their interaction with secondary aerosol formation remain uncertain. Sulfate formation linearly increased with SO<sub>2</sub> concentration when VOCs and NO<sub>x</sub> did not vary [13], but it varied with the var-

ying VOCs concentration [25]. Oxidation of SO<sub>2</sub> seemed to have little effect on the concentrations of free radicals in the photooxidation of VOCs and NO<sub>x</sub> [13], but may enhance SOA formation through acid-catalyzed heterogeneous reactions [13,14]. However, nitrate formation seemed to be also related to the presence of SO<sub>2</sub> [25]. Recently, oxidation of SO<sub>2</sub> by Criegee intermediates has been a wide concern [26,27]. The chemistry in the oxidation of VOCs may play a vital role in sulfate formation. A uniform explanation for these phenomena should be developed for a better understanding of the complex chemistry in haze formation.

In this study, we carried out a series of smog chamber experiments to investigate secondary aerosol formation from photooxidation of VOCs/NO<sub>x</sub>/SO<sub>2</sub>/NH<sub>3</sub> under atmospheric conditions. To understand the controlling factors of secondary aerosols formation and oxidation capacity, their sensitivity to NO<sub>x</sub> and hydrocarbon precursors in the presence or absence of mineral seed particles (Al<sub>2</sub>O<sub>3</sub>) and inorganic gas pollutants (SO<sub>2</sub> and NH<sub>3</sub>) is discussed.

## 2 Methods

Two smog chambers were used in this study. The first one is a chamber with a 30 m<sup>3</sup> reactor made of FEP Teflon film (FEP 100, Type 200A; DuPont, USA) with a surface-to-volume ratio of 2.1 m<sup>-1</sup>. The chamber has been described in detail by Wang *et al.* [28]. The enclosure temperature of the chamber is controlled by three cooling units and a heater. A total of 135 black lamps (1.2 m long, 60 W Philips/10R BL; Royal Dutch Philips Electronics Ltd., Netherlands) are arranged in two banks to provide irradiation during the experiments. Ozone and NO<sub>x</sub> (NO and NO<sub>2</sub>) were measured by an ozone analyzer (EC9810, Ecotech, Australia) and a chemiluminescence analyzer (EC9841T, Ecotech, Australia), respectively. VOCs inside of the reactor were measured by both a preconcentrator (Model 7100, Entech Instruments Inc., USA) coupled with a gas chromatography-mass selective detector/flame ionization detector/electron capture detector (GC-MSD/FID/ECD, Agilent 5973N, Agilent Technologies, USA) and a proton-transfer-reaction time-of-flight mass spectrometer (PTR-TOF-MS, Ionicon Analytik GmbH, Austria). A scanning mobility particle sizer (SMPS) equipped with a differential mobility analyzer (TSI 3081, TSI Incorporated, USA) coupled with a condensation particle counter (TSI 3775, TSI Incorporated, USA) and a high-resolution time-of-flight aerosol mass spectrometer (HR-TOF-MS, Aerodyne Research Incorporated, USA) were used to measure the size distributions and chemical compositions of the particles, respectively. Wall deposition of particles in the chamber was corrected with the method developed by Pathak *et al.* [29], which was also described in Wang *et al.* [28].

The second chamber is a small 2 m<sup>3</sup> cuboid reactor constructed with 50 μm-thick FEP-Teflon film (Toray Indus-

tries, Inc., Japan), with a surface-to-volume ratio of  $5 \text{ m}^{-1}$ . The chamber was described in detail in Wu *et al.* [30]. A temperature-controlled enclosure (SEWT-Z-120, Escpec, Japan) provides a constant temperature between 10 and  $30 \text{ }^\circ\text{C}$  ( $\pm 0.5 \text{ }^\circ\text{C}$ ), and 40 black lights (GE F40T12/BLB, peak intensity at 365 nm, General Electric Company, USA) provide irradiation during the experiments. The hydrocarbon concentration was measured by a gas chromatograph (GC, Beifen SP-3420, Beifen, China) equipped with a DB-5 column ( $30 \text{ m} \times 0.53 \text{ mm} \times 1.5 \text{ mm}$ , Dikma, USA) and flame ionization detector (FID), while  $\text{NO}_x$  and  $\text{O}_3$  were monitored by an  $\text{NO}_x$  analyzer (Model 42C, Thermo Environmental Instruments, USA) and an  $\text{O}_3$  analyzer (Model 49C, Thermo Environmental Instruments, USA), respectively. An SMPS (TSI 3936, TSI Incorporated, USA) was used to measure the size distribution of particulate matter (PM) in the chamber, and also employed to estimate the volume and mass concentration. The chemical composition of aerosols was measured by an aerosol chemical speciation monitor (ACSM, Aerodyne Research Incorporated, USA). ACSM is a simplified version of aerosol mass spectrometry (AMS), with similar principles and structure. Ng *et al.* [31] presented a detailed introduction to this instrument and found that the measurement results agreed well with AMS. Wall deposition of particles in the chamber was similarly corrected as in the first chamber by using a regression equation to describe the dependence of deposition rate on the particle size [15]. And the detailed information about the equation was described in our previous studies [10,32]. Using the regression equation had very limited influence on particle concentrations (less than 1% for mean value).

Alumina seed particles were produced on-line via a spray pyrolysis setup, which has been described in detail elsewhere [33]. Liquid aluminol ( $\text{AlOOH}$ , Lot No. 2205, Kawaken Fine Chemicals Co., Ltd., Japan) with an initial concentration of 1.0 wt%, which was calculated according to  $\text{Al}_2\text{O}_3$  content, was adopted as the precursor solution. Aluminol was sprayed to droplets by an atomizer and carried through the diffusion dryer to remove water. The partly dried droplets were then carried into the corundum tube embedded in the tubular furnace with the temperature maintained at  $1000 \text{ }^\circ\text{C}$ . Eventually, the generated alumina

particles were introduced into the chamber through a neutralizer. The obtained alumina particles were  $\gamma\text{-Al}_2\text{O}_3$  as detected by X-ray diffraction measurements, and spherical-shaped according to electron micrograph results. In addition, toluene and  $\alpha$ -pinene were injected into a vaporizer and then carried into the chamber by purified air, while  $\text{NO}_x$ ,  $\text{SO}_2$  and  $\text{NH}_3$  were directly injected into the chamber from the standard gas bottles.

### 3 Results and discussion

#### 3.1 Sensitivity of secondary aerosol formation to $\text{NO}_x$ under “VOC-limited” and “ $\text{NO}_x$ -limited” conditions

Aerosol formation in the toluene/ $\text{NO}_x$ / $\text{SO}_2$  photooxidation experiments was investigated under both “VOC-limited” and “ $\text{NO}_x$ -limited” conditions. Toluene was selected in these experiments as a representative hydrocarbon from anthropogenic emissions. The detailed experimental conditions are listed in Table 1. The first four experiments in Table 1 were carried out in the  $30 \text{ m}^3$  chamber at 50% relative humidity (RH) and  $25 \text{ }^\circ\text{C}$  to simulate particle formation under “VOC-limited” conditions. In these four experiments, the concentrations of  $\text{NO}_x$  were either lower than 100 ppb or higher than 200 ppb, with the corresponding C/N atomic ratios of about 2 and 7, respectively. The concentrations of toluene and  $\text{SO}_2$  were similar in these experiments. The concentration of toluene was designed to be relatively low compared with  $\text{NO}_x$  to simulate “VOC-limited” conditions. The first two experiments were carried out in the absence of  $\text{Al}_2\text{O}_3$  seed particles and were referred as seed-free experiments in which the background particle number concentration was less than  $5 \text{ particles m}^{-3}$ , while the other two were referred as seed-introduced experiments, which carried out in the presence of thousands of  $\text{Al}_2\text{O}_3$  seed particles. Similarly, the other four experiments in Table 1 were conducted to simulate particle formation under “ $\text{NO}_x$ -limited” conditions. High concentrations of toluene were introduced in these four experiments, while the corresponding C/N atomic ratios were about 35 and 70 in experiments with a low and high concentration of  $\text{NO}_x$ , respectively. These four

**Table 1** Experimental conditions for photooxidation of toluene/ $\text{NO}_x$ / $\text{SO}_2$  under “VOC-limited” and “ $\text{NO}_x$ -limited” conditions

	No.	Toluene (ppb)	$\text{NO}_x$ (ppb)	C/N	$\text{Al}_2\text{O}_3$ seed particles		$\text{SO}_2$ (ppb)
					Number ( $\text{particles m}^{-3}$ )	Volume ( $\mu\text{m}^3 \text{ cm}^{-3}$ )	
“VOC-limited”	N69	79.6	69	8.1	~0	~0	104
	N221	75.5	221	2.4	~0	~0	99
	AIN86	75.8	86	6.2	~3100	12.9	125
	AIN277	75.9	277	1.9	~3400	13.2	120
“ $\text{NO}_x$ -limited”	N105	1050	105	70.0	~0	~0	137
	N206	1020	206	34.7	~0	~0	138
	AIN104	1110	104	74.7	~6300	53.6	140
	AIN205	1030	205	35.2	~6200	53.3	134

experiments were carried out in the 2 m<sup>3</sup> chamber at 50% RH and 30 °C. Considering that the temperatures were a little different in the two chambers, we only directly compared particle formation in the contrast experiments carried out in the same chamber, while the effects of temperature and humidity on the sensitivity of secondary aerosol formation to NO<sub>x</sub> would be discussed in Section 3.3.

For the “VOC-limited” experiments, increasing NO<sub>x</sub> concentration suppressed the secondary aerosol formation in both the seed-free experiments and the seed-introduced experiments. Time variations of concentration of the generated PM in these experiments are shown in Figure 1(a). Particle density was assumed to be 1.4 g cm<sup>-3</sup> in this study, following previous work [10,34–36]. We also measured the chemical composition of the generated aerosols after 6 h of photooxidation in each experiment with the AMS as shown in Figure 1(b). Less SOA, nitrate and sulfate were generated with the increasing NO<sub>x</sub> concentration, indicating a decreased oxidation capacity which resulted in a slower transition of SO<sub>2</sub> to sulfate in the experiments. The oxidation in both homogeneous and heterogeneous reactions was included here, since both the two processes could lead to the formation of sulfate. According to the decay of the VOC species, the concentration of gas phase OH radical was estimated to be decreasing from 2.83×10<sup>6</sup> to 1.78×10<sup>6</sup> molecule cm<sup>-3</sup> in the seed-free experiments, and from 1.01×10<sup>6</sup> to 9.78×10<sup>5</sup> molecule cm<sup>-3</sup> in the seed-introduced experiments with the increasing NO<sub>x</sub> concentration, which con-

firmed that the oxidation capacity decreased at a higher NO<sub>x</sub> concentration in the reaction system. The dependence of SOA formation with NO<sub>x</sub> in the presence of SO<sub>2</sub> was consistent with the widely observed lower SOA yield for lower VOC/NO<sub>x</sub> ratios [22,23,37,38]. Nitrate formation was detected in the seed-free experiments without introducing NH<sub>3</sub> into the reactor. Nitrate generation in these experiments in NH<sub>3</sub>-poor environments was consistent with the observation results in Beijing and Shanghai, China [9]. Nitrate was proposed to be generated via heterogeneous hydrolysis of N<sub>2</sub>O<sub>5</sub> on the surface of moist and acidic aerosols in an NH<sub>3</sub>-poor environment [9].

To confirm the dependence of secondary aerosol formation on oxidation capacity with different VOC/NO<sub>x</sub> ratios under “VOC-limited” conditions, we further studied the effects of hydrocarbon concentration on secondary aerosol formation. In the presence of Al<sub>2</sub>O<sub>3</sub> seed particles, three experiments with similar NO<sub>x</sub> concentrations but different toluene concentrations were carried out at 80% RH and 12 °C. In these three experiments, increasing tendencies for all the major chemical species were observed with the increasing toluene concentrations, as shown in Figure 2, which indicated a dependence of oxidation capacity on the hydrocarbon concentration rather than NO<sub>x</sub>. This was supported by the oxidation level of the generated organic aerosol, as shown in Figure 2. The atomic ratio of oxygen to carbon (O/C) of the organic aerosol increased with the increasing toluene concentration. Generally, organic aerosol

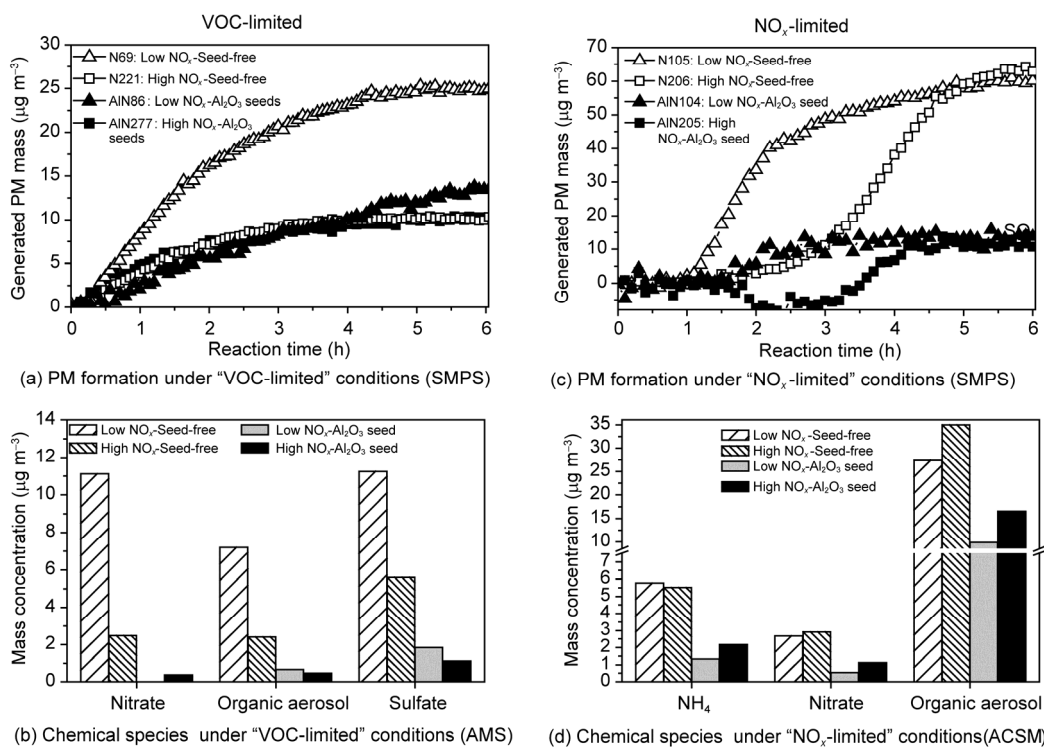


**Figure 1** Secondary aerosol generation and chemical species concentrations (after 6 h of reaction) in photooxidation of toluene/NO<sub>x</sub>/SO<sub>2</sub> under “VOC-limited” (a, b) and “NO<sub>x</sub>-limited” conditions (c, d).

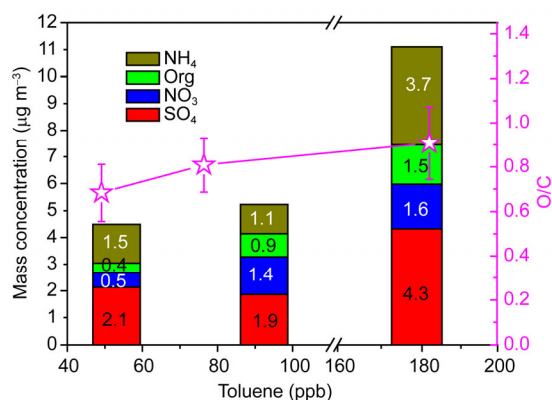


**Figure 2** Particle formation and the oxidation level of organic aerosol after 5 h of reaction in photooxidation with various concentrations of toluene under “VOC-limited” conditions.

was oxidized more, which resulted in a higher O/C ratio, with lower concentrations of hydrocarbon precursor [39,40]. Here, the increasing O/C ratio with the increasing toluene confirmed that these experiments were carried out under “VOC-limited” conditions and that the oxidation capacity was highly sensitive to the hydrocarbon concentration. Thus the change of O/C ratio in organic aerosols might be used as one indicator to estimate the oxidation capacity and then to distinguish the “VOC-limited” and “NO<sub>x</sub>-limited” conditions.

The response of aerosol formation to the NO<sub>x</sub> concentration was different under “NO<sub>x</sub>-limited” conditions compared with the “VOC-limited” experiments. The concentrations of generated PM measured by the SMPS in experiments with different concentrations of NO<sub>x</sub> were similar under “NO<sub>x</sub>-limited” conditions, as shown in Figure 1(c). But after 6-h reaction, the main components in the generated PM measured by the ACSM were all slightly more in experiments with higher concentrations of NO<sub>x</sub>, as displayed in Figure 1(d). This discrepancy between the SMPS and the ACSM results might be reached by inaccurate estimations of wall deposition in SMPS measurement since the particle volume decreased in the first few hours in the experiment with Al<sub>2</sub>O<sub>3</sub> seed particles and a high concentration of NO<sub>x</sub>. An increasing oxidizing capacity dependent on NO<sub>x</sub> concentration was observed since the formation of both organic aerosol and sulfate increased with the increasing NO<sub>x</sub>. Sulfate formation could be enhanced by NO<sub>2</sub> in the aqueous aerosol suspensions [41] and on the surface of mineral oxides [42] or sandstone [43]. Heterogeneous might occur and contributed to sulfate formation in these experiments. The effect of NO<sub>x</sub> on SOA yields is complex. Under high NO<sub>x</sub> conditions, organo-peroxy radicals (RO<sub>2</sub>) react with NO and NO<sub>2</sub> instead of with peroxy radicals (RO<sub>2</sub> or HO<sub>2</sub>), resulting in the formation of volatile organic products and a decreased SOA yield [23,38]. However, SOA yield increased with the increasing concentration of NO<sub>x</sub> in these experiments under “NO<sub>x</sub>-limited” conditions. Differing NO<sub>x</sub> levels were pro-

posed to impact the heterogeneous reactions in the aerosol [22,44], and might be the reason for the increasing SOA formation in Figure 1(d). Besides, the presence of SO<sub>2</sub> might also contribute to SOA formation in the acid-catalyzed heterogeneous reactions [13,14]. Nitrate formation also increased with the increasing NO<sub>x</sub>, but the increase was much less than NO<sub>x</sub>, indicating that most nitric acid was restricted in the gas phase. The high concentration of NO<sub>x</sub> delayed the formation of secondary aerosol (dominated by SOA), in which the gas phase oxidation limited the formation rate of organic aerosol. This phenomenon was not observed in the “VOC-limited” experiments. The presence of Al<sub>2</sub>O<sub>3</sub> seed particles decreased the particle formation in photooxidation of toluene/NO<sub>x</sub>/SO<sub>2</sub>, especially in the experiments with low concentrations of NO<sub>x</sub>. Sulfate, nitrate and SOA mass all decreased in experiments in the presence of Al<sub>2</sub>O<sub>3</sub> seed particles compared with the seed-free experiments, indicating a decrease of oxidation capacity caused by Al<sub>2</sub>O<sub>3</sub> seed particles. Liu *et al.* [45] reported that Al<sub>2</sub>O<sub>3</sub> seed particles only resulted in a slight reduction of SOA yield compared with a seed-free system in photooxidation of  $\alpha$ -pinene/NO<sub>x</sub>. It was speculated that Al<sub>2</sub>O<sub>3</sub> seed particles decreased the O<sub>3</sub> concentration and therefore suppressed SOA formation from  $\alpha$ -pinene ozonolysis. Here, a more significant reduction (about 50%–80%) of SOA formation caused by Al<sub>2</sub>O<sub>3</sub> seed particles was observed in photooxidation of toluene/NO<sub>x</sub>/SO<sub>2</sub>. However, in experiments without SO<sub>2</sub>, the presence of Al<sub>2</sub>O<sub>3</sub> seed particles had no obvious suppressing effect on the secondary aerosol formation in photooxidation of toluene/NO<sub>x</sub>, as shown in Figure 3. One possible reason for these phenomena was the uptake of sulfuric acid, which was generated from the oxidation of the co-existing SO<sub>2</sub>, on the Al<sub>2</sub>O<sub>3</sub> seed particles. It is well known that acid aerosols can enhance SOA formation through acid-catalyzed heterogeneous reactions [13,14]. This enhancement effect might be weakened in the presence of Al<sub>2</sub>O<sub>3</sub> seed particles due to its amphoteric characteristics, resulting in less SOA formation. This hypothesis was further supported by the experiments carried out in the presence of NH<sub>3</sub> in Figure 3. The concentration of the NH<sub>3</sub> was calculated to be about 260 ppb according to the volume of the injected NH<sub>3</sub> and the reactor. With the sulfuric acid neutralized by NH<sub>3</sub>, Al<sub>2</sub>O<sub>3</sub> seed particles had no obvious suppressing effect on the secondary aerosol formation. It is necessary to point out that the particle volume decreased in experiment “AIN205” with Al<sub>2</sub>O<sub>3</sub> seed particles and a high concentration of NO<sub>x</sub>. This might indicate an underestimation of wall deposition or a physicochemical property change of the Al<sub>2</sub>O<sub>3</sub> seed particles, resulting in an exaggerated effect of the particles on secondary aerosol formation. It was also possible that some particles larger than 1  $\mu$ m, which exceeded the measuring ranges of the SMPS system, were generated in this experiment and therefore led to an underestimate of the particle concentration.

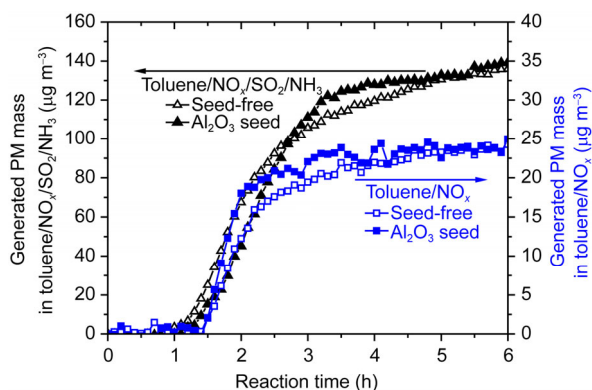


**Figure 3** Particle formation in photooxidation of toluene/NO<sub>x</sub>/SO<sub>2</sub>/NH<sub>3</sub> and toluene/NO<sub>x</sub> in the presence or absence of Al<sub>2</sub>O<sub>3</sub> seed particles.

### 3.2 Effects of NO<sub>x</sub> concentration on the secondary aerosol formation under homogeneous and heterogeneous conditions

The presence of Al<sub>2</sub>O<sub>3</sub> seed particles also seemed to influence the sensitivity of the secondary aerosol formation to NO<sub>x</sub> concentration. As shown in Figure 1, under “VOC-limited” conditions, the increasing NO<sub>x</sub> concentration resulted in a less significant decrease of the secondary aerosol formation in seed-introduced experiments (decrease 25%) than that in seed-free experiments (decrease 59%). Under “NO<sub>x</sub>-limited” conditions, however, increasing NO<sub>x</sub> concentration resulted in 58% more secondary aerosol formation in seed-introduced experiments, which is higher than

that in seed-free experiments (increase 21%), as shown in Figure 1(d). This indicated a synergetic promoting effect of mineral dust and NO<sub>x</sub> on secondary aerosol formation. This effect strengthened the positive relationship between NO<sub>x</sub> and the secondary aerosol formation under “NO<sub>x</sub>-limited” conditions, but weakened their negative relationship under “VOC-limited” conditions.

To confirm this promoting effect, α-pinene was further selected as a representative hydrocarbon from biogenic emissions to simulate particle formation under “NO<sub>x</sub>-limited” conditions with different concentrations of NO<sub>x</sub>. The experimental conditions were similar to that of the toluene experiment except that a different hydrocarbon was used; the details can be found in Table 2. Time variations of PM formation in the four α-pinene experiments are shown in Figure 4(a). In these experiments, the effects of NO<sub>x</sub> on PM formation were opposite between the seed-free experiments and the seed-introduced experiments. Much less PM was generated with higher concentrations of NO<sub>x</sub> in the seed-free experiments, as shown in Figure 4(b). This is consistent with previous studies showing that SOA yield decreased with increasing NO<sub>x</sub> [22]. However, in the experiments in the presence of Al<sub>2</sub>O<sub>3</sub> seed particles, the increasing NO<sub>x</sub> resulted in a significant increase in SOA and sulfate formation, as shown in Figure 4(b). The promoting effects of mineral dust and NO<sub>x</sub> on the oxidation of SO<sub>2</sub> were reported [1,42]. It seemed that mineral dust and NO<sub>x</sub> together promoted SOA formation in the photooxidation of α-pinene/NO<sub>x</sub>/SO<sub>2</sub>, in which heterogeneous reactions may

**Table 2** Experimental condition for photooxidation of α-pinene/NO<sub>x</sub>/SO<sub>2</sub> under “NO<sub>x</sub>-limited” conditions<sup>a)</sup>

NO.	α-Pinene (ppm)	NO <sub>x</sub> (ppb)	C/N	Al <sub>2</sub> O <sub>3</sub> seed particle		SO <sub>2</sub> (ppb)
				Number (particles m <sup>-3</sup> )	Volume (µm <sup>3</sup> cm <sup>-3</sup> )	
N50	0.20	95	21.1	~0	~0	136
N150	0.19	197	9.6	~0	~0	136
AIN50	0.20	99	20.2	~7100	45.5	137
AIN150	0.20	208	9.6	~5600	41.2	139

a) Experiments were carried out at 50% RH and 30 °C.

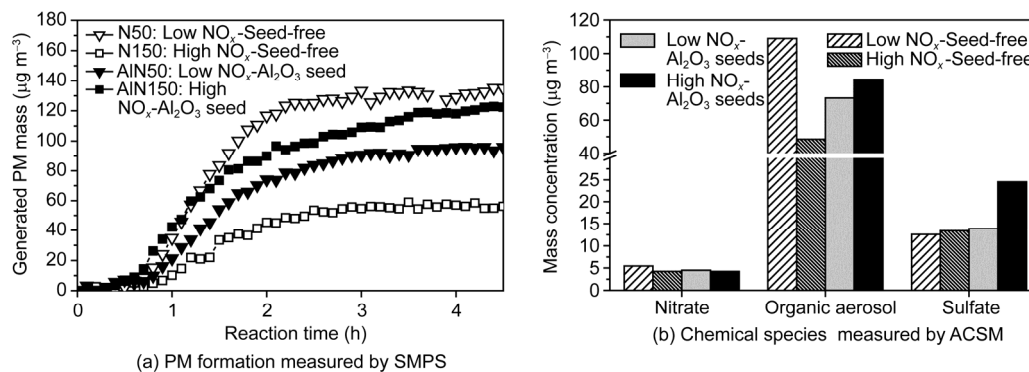


**Figure 4** Secondary aerosol generation and chemical species concentrations after 4.5 h of reaction in photooxidation of α-pinene/NO<sub>x</sub>/SO<sub>2</sub> under “NO<sub>x</sub>-limited” conditions.

have played an important role. These experimental results also indicated that the sensitivity of secondary aerosol formation to  $\text{NO}_x$  might be different under homogeneous and heterogeneous conditions. The high concentration of  $\text{NO}_x$  suppressed SOA formation in homogeneous reactions with organo-peroxy radicals ( $\text{RO}_2$ ), but enhance the secondary aerosol formation in heterogeneous reactions, which might be very important in heavy haze pollution. The synergetic effect of mineral dust and  $\text{NO}_x$  on the secondary aerosol formation in heterogeneous reactions should be considered in air quality models for a better understanding of heavy haze pollution [46].

### 3.3 Sensitivity of secondary aerosol formation to $\text{NO}_x$ under “winter-like” and $\text{NH}_3$ -rich conditions

Heavy haze pollution in eastern China usually occurs in winter, characterized by a low temperature, high RH and a low light intensity. The secondary aerosol formation under “winter-like” conditions was also simulated in this study. Due to the low reactivity of toluene, particle formation under “winter-like” conditions was not significant in photooxidation of toluene/ $\text{NO}_x$ / $\text{SO}_2$ , and therefore, it was not easy to estimate the sensitivity of secondary aerosol formation to  $\text{NO}_x$ .  $\text{NH}_3$  is an important gas phase pollutant in the atmosphere, and was used in this study to enhance the particle formation and to simulate the secondary aerosol formation in an  $\text{NH}_3$ -rich environment.  $\text{NH}_3$  neutralizes sulfuric acid and nitric acid, and forms ammonia sulfate and ammonia nitrate, both of which are main components of  $\text{PM}_{2.5}$  in the atmosphere. The secondary inorganic aerosol formation is closely related to the abundance of  $\text{NH}_3$  gas [9,16,17], while SOA formation was also found to be increased in the presence of  $\text{NH}_3$  [47]. Two photooxidation experiments carried out under “winter-like” conditions are listed in Table 3. These two experiments were carried out at 80% RH and 10 °C in the 2 m<sup>3</sup> chamber, for which only a quarter of the black lights (10 lights) were turned on in the reaction. The  $\text{NH}_3$  concentration was not directly measured because of the lack of an online instrument in our laboratory, but was estimated to be about 260 ppb according to the volume of the injected  $\text{NH}_3$  and the reactor. The calculated concentration of  $\text{NH}_3$  was designed to be higher than that of  $\text{SO}_2$  to simulate the secondary aerosol formation in an  $\text{NH}_3$ -rich environment. The C/N atomic ratios were designed to be about 60 and 30 in experiments with low or high concentration of  $\text{NO}_2$ , respectively, to simulate the “ $\text{NO}_x$ -limited” conditions.

Both of the experiments were carried out in the presence of thousands of  $\text{Al}_2\text{O}_3$  seed particles.

The time variation of the aerosol concentration in these two experiments and the chemical composition of the generated aerosols are displayed in Figure 5. Under the conditions of these two experiments, aerosol formation was enhanced by increasing  $\text{NO}_x$  concentration. All the chemical species, including sulfate, organic aerosol, nitrate and ammonia, were generated in higher amounts. At a lower temperature and higher RH, an increase of sulfate and organic aerosol formation similar to that at a higher temperature and lower RH conditions was observed. Slightly more sulfate (about 2  $\mu\text{g m}^{-3}$ ) and organic aerosol (about 4  $\mu\text{g m}^{-3}$ ) were generated with the increasing  $\text{NO}_x$  concentration under both of the two different environmental conditions. However, increasing  $\text{NO}_x$  resulted in a more significant increase of nitrate formation under “winter-like” and  $\text{NH}_3$ -rich conditions, as shown in the right part of Figure 5. In the experiment with a high concentration of  $\text{NO}_x$ , the concentration of ammonium nitrate was about 3 times as high as that in the experiment with a low concentration of  $\text{NO}_x$ . This was consistent with our earlier observation that most nitric acid was restricted in the gas phase in an  $\text{NH}_3$ -poor environment. The increased ratio of nitrate was higher than that of  $\text{NO}_x$ , being consistent with the increased oxidation capacity which enhanced the transition of  $\text{NO}_x$  to nitric acid. The response of the secondary species with the concentration of  $\text{NO}_x$  indicated that the presence of  $\text{NH}_3$ , different temperatures and RHs had no obvious effect on the sensitivity of the oxidation capacity to  $\text{NO}_x$  concentration, but influenced the sensitivity of nitrate formation to  $\text{NO}_x$  concentration.

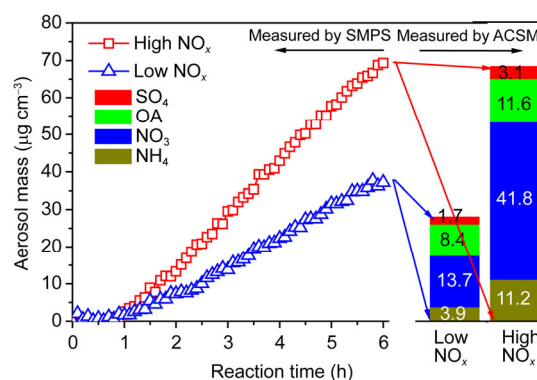


**Figure 5** Particle formation in photooxidation of toluene/ $\text{NO}_x$ / $\text{SO}_2$ / $\text{NH}_3$  under “ $\text{NO}_x$ -limited” and “winter-like” conditions.

**Table 3** Experimental conditions for photooxidation of toluene/ $\text{NO}_x$ / $\text{SO}_2$ / $\text{NH}_3$  under the “winter-like” and “ $\text{NO}_x$ -limited” conditions

NO.	Toluene (ppm)	$\text{NO}_x$ (ppb)	C/N	$\text{Al}_2\text{O}_3$ seed particle		$\text{SO}_2$ (ppb)
				Number (particles $\text{m}^{-3}$ )	Volume ( $\mu\text{m}^3 \text{cm}^{-3}$ )	
Low $\text{NO}_x$	1.18	139	59.4	1400	9.3	134
High $\text{NO}_x$	1.13	268	29.5	1900	11.7	141

## 4 Conclusions

The experimental results of the secondary aerosol formation in photooxidation of toluene/NO<sub>x</sub>/air and  $\alpha$ -pinene/NO<sub>x</sub>/air showed that the secondary aerosol formation was suppressed with the increasing NO<sub>x</sub> concentration under “VOC-limited” conditions, while it was enhanced under “NO<sub>x</sub>-limited” conditions. Considering both the homogenous and heterogeneous reactions, the oxidation capacity decreased with increasing NO<sub>x</sub> concentration under “VOC-limited” conditions, but was highly sensitive to the VOC precursor concentration. With the increasing toluene concentration, both the organic aerosol mass and the oxidation degree of the organic aerosol increased. The tendency of the formation of sulfate, nitrate and SOA was consistent with the change of the oxidation capacity with NO<sub>x</sub> and hydrocarbon concentration in the photochemical process. The chemistry about the reactions between NO<sub>x</sub> and RO<sub>2</sub> cannot fully explain the suppressing effect of NO<sub>x</sub> on SOA formation, while heterogeneous reactions might play an important role. Sensitivity of the secondary aerosol formation to NO<sub>x</sub> seemed different in homogeneous and heterogeneous reactions, and should be both taken into account. In the presence of Al<sub>2</sub>O<sub>3</sub> seed particles, there was a synergetic promoting effect of mineral dust and NO<sub>x</sub> on the secondary aerosol formation in heterogeneous reactions. This synergetic effect strengthened the enhancing effect of NO<sub>x</sub> on the secondary aerosol formation under “NO<sub>x</sub>-limited” conditions, but weakened or even overturned the suppressing effect of NO<sub>x</sub> on the secondary aerosol formation under “VOC-limited” conditions. The synergetic effect of mineral dust and NO<sub>x</sub> on the secondary aerosol formation in heterogeneous reactions should be considered in air quality models for a better understanding of heavy haze pollution. The presence of NH<sub>3</sub>, different temperatures and RHs had no obvious effect on the sensitivity of the formation of sulfate and organic aerosol to NO<sub>x</sub> concentration, but influenced nitrate formation. Much more nitrate was generated in experiments at a lower temperature and in the presence of NH<sub>3</sub>. Meanwhile, a more significant increase of nitrate formation with the increasing NO<sub>x</sub> was also observed, which indicated that the presence of NH<sub>3</sub> might play an important role in the secondary aerosol formation in winter haze.

This work was supported by the National Natural Science Foundation of China (21407158) and the “Strategic Priority Research Program” of the Chinese Academy of Sciences (XDB05010300, XDB05040100, XDB05010200).

- 1 He H, Wang Y, Ma Q, Ma J, Chu B, Ji D, Tang G, Liu C, Zhang H, Hao J. Mineral dust and NO<sub>x</sub> promote the conversion of SO<sub>2</sub> to sulfate in heavy pollution days. *Sci Rep*, 2014, 4: 04172
- 2 Yang F, Tan J, Zhao Q, Du Z, He K, Ma Y, Duan F, Chen G, Zhao Q. Characteristics of PM<sub>2.5</sub> speciation in representative megacities and across China. *Atmos Chem Phys*, 2011, 11: 5207–5219

- 3 Zhao PS, Dong F, He D, Zhao XJ, Zhang XL, Zhang WZ, Yao Q, Liu HY. Characteristics of concentrations and chemical compositions for PM<sub>2.5</sub> in the region of Beijing, Tianjin, and Hebei, China. *Atmos Chem Phys*, 2013, 13: 4631–4644
- 4 Dan M, Zhuang G, Li X, Tao H, Zhuang Y. The characteristics of carbonaceous species and their sources in PM<sub>2.5</sub> in Beijing. *Atmos Environ*, 2004, 38: 3443–3452
- 5 Duan F, He K, Ma Y, Jia Y, Yang F, Lei Y, Tanaka S, Okuta T. Characteristics of carbonaceous aerosols in Beijing, China. *Chemosphere*, 2005, 60: 355–364
- 6 Wang Z, Wang T, Guo J, Gao R, Xue L, Zhang J, Zhou Y, Zhou X, Zhang Q, Wang W. Formation of secondary organic carbon and cloud impact on carbonaceous aerosols at Mount Tai, north China. *Atmos Environ*, 2012, 46: 516–527
- 7 Wang Y, Yao L, Wang L, Liu Z, Ji D, Tang G, Zhang J, Sun Y, Hu B, Xin J. Mechanism for the formation of the January 2013 heavy haze pollution episode over central and eastern China. *Sci China Earth Sci*, 2014, 57: 14–25
- 8 Wilkins ET. Air pollution aspects of the London fog of December 1952. *Quart J Roy Meteor Soc*, 1954, 80: 267–271
- 9 Pathak RK, Wu WS, Wang T. Summertime PM<sub>2.5</sub> ionic species in four major cities of China: nitrate formation in an ammonia-deficient atmosphere. *Atmos Chem Phys*, 2009, 9: 1711–1722
- 10 Chu B, Liu Y, Li J, Takekawa H, Liggio J, Li SM, Jiang J, Hao J, He H. Decreasing effect and mechanism of FeSO<sub>4</sub> seed particles on secondary organic aerosol in  $\alpha$ -pinene photooxidation. *Environ Pollut*, 2014, 193: 88–93
- 11 Jang MS, Czoschke NM, Lee S, Kamens RM. Heterogeneous atmospheric aerosol production by acid-catalyzed particle-phase reactions. *Science*, 2002, 298: 814–817
- 12 Zhu T, Shang J, Zhao DF. The roles of heterogeneous chemical processes in the formation of an air pollution complex and gray haze. *Sci China Chem*, 2011, 54: 145–153
- 13 Kleindienst TE, Edney EO, Lewandowski M, Offenberg JH, Jaoui M. Secondary organic carbon and aerosol yields from the irradiations of isoprene and  $\alpha$ -pinene in the presence of NO<sub>x</sub> and SO<sub>2</sub>. *Environ Sci Technol*, 2006, 40: 3807–3812
- 14 Santiago M, Garcia Vivanco M, Stein AF. SO<sub>2</sub> effect on secondary organic aerosol from a mixture of anthropogenic VOCs: experimental and modelled results. *Int J Environ Pollut*, 2012, 50: 224–233
- 15 Takekawa H, Minoura H, Yamazaki S. Temperature dependence of secondary organic aerosol formation by photo-oxidation of hydrocarbons. *Atmos Environ*, 2003, 37: 3413–3424
- 16 Derwent R, Witham C, Redington A, Jenkin M, Stedman J, Yardley R, Hayman G. Particulate matter at a rural location in southern England during 2006: model sensitivities to precursor emissions. *Atmos Environ*, 2009, 43: 689–696
- 17 Vingarzan R, Li SM. The Pacific 2001 air quality study—synthesis of findings and policy implications. *Atmos Environ*, 2006, 40: 2637–2649
- 18 Kelly NA, Gunst RF. Response of ozone to changes in hydrocarbon and nitrogen-oxide concentrations in outdoor smog chambers filled with Los Angeles air. *Atmos Environ A*, 1990, 24: 2991–3005
- 19 Seinfeld JH, Pandis SN. *Atmospheric Chemistry and Physics: from Air Pollution to Climate Change*. Weinheim: John Wiley & Sons, Inc., 2006
- 20 Qi Q, Zhou XH, Wang WX. Studies on formation of aqueous secondary organic aerosols. *Prog Chem*, 2014, 26: 458–466
- 21 Wang Z, Wang T, Gao R, Xue LK, Guo J, Zhou Y, Nie W, Wang XF, Xu PJ, Gao JA, Zhou XH, Wang WX, Zhang QZ. Source and variation of carbonaceous aerosols at Mount Tai, north China: results from a semi-continuous instrument. *Atmos Environ*, 2011, 45: 1655–1667
- 22 Song C, Na KS, Cocker DR. Impact of the hydrocarbon to NO<sub>x</sub> ratio on secondary organic aerosol formation. *Environ Sci Technol*, 2005, 39: 3143–3149



- 23 Lane TE, Donahue NM, Pandis SN. Effect of  $\text{NO}_x$  on secondary organic aerosol concentrations. *Environ Sci Technol*, 2008, 42: 6022–6027
- 24 Wang BB, Laskin A. Reactions between water-soluble organic acids and nitrates in atmospheric aerosols: recycling of nitric acid and formation of organic salts. *J Geophys Res-Atmos*, 2014, 119: 3335–3351
- 25 Jaoui M, Edney EO, Kleindienst TE, Lewandowski M, Offenbergh JH, Surratt JD, Seinfeld JH. Formation of secondary organic aerosol from irradiated alpha-pinene/toluene/ $\text{NO}_x$  mixtures and the effect of isoprene and sulfur dioxide. Formation of secondary organic aerosol from irradiated alpha-pinene/toluene/ $\text{NO}_x$  mixtures and the effect of isoprene and sulfur dioxide. *J Geophys Res-Atmos*, 2008, 113: D9
- 26 Welz O, Savee JD, Osborn DL, Vasu SS, Percival CJ, Shallcross DE, Taatjes CA. Direct kinetic measurements of criegee intermediate ( $\text{CH}_2\text{OO}$ ) formed by reaction of  $\text{CH}_2\text{I}$  with  $\text{O}_2$ . *Science*, 2012, 335: 204–207
- 27 Mauldin RL, Berndt T, Sipila M, Paasonen P, Petaja T, Kim S, Kurten T, Stratmann F, Kerminen VM, Kulmala M. A new atmospherically relevant oxidant of sulphur dioxide. *Nature*, 2012, 488: 193–196
- 28 Wang X, Liu T, Bernard F, Ding X, Wen S, Zhang Y, Zhang Z, He Q, Lu S, Chen J, Saunders S, Yu J. Design and characterization of a smog chamber for studying gas-phase chemical mechanisms and aerosol formation. *Atmos Meas Tech*, 2014, 7: 301–313
- 29 Pathak RK, Stanier CO, Donahue NM, Pandis SN. Ozonolysis of alpha-pinene at atmospherically relevant concentrations: temperature dependence of aerosol mass fractions (yields). *J Geophys Res-Atmos*, 2007, 112: D03201
- 30 Wu S, Lu ZF, Hao JM, Zhao Z, Li JH, Hideto T, Hiroaki M, Akio Y. Construction and characterization of an atmospheric simulation smog chamber. *Adv Atmos Sci*, 2007, 24: 250–258
- 31 Ng NL, Herndon SC, Trimborn A, Canagaratna MR, Croteau PL, Onasch TB, Sueper D, Worsnop DR, Zhang Q, Sun YL, Jayne JT. An aerosol chemical speciation monitor (ACSM) for routine monitoring of the composition and mass concentrations of ambient aerosol. *Aerosol Sci Technol*, 2011, 45: 770–784
- 32 Chu B, Hao J, Takekawa H, Li J, Wang K, Jiang J. The remarkable effect of  $\text{FeSO}_4$  seed aerosols on secondary organic aerosol formation from photooxidation of  $\alpha$ -pinene/ $\text{NO}_x$  and toluene/ $\text{NO}_x$ . *Atmos Environ*, 2012, 55: 26–34
- 33 Liu C, Liu Y, Ma Q, He H. Mesoporous transition alumina with uniform pore structure synthesized by aluminol spray pyrolysis. *Chem Eng J*, 2010, 163: 133–142
- 34 Alfarra MR, Paulsen D, Gysel M, Garforth AA, Dommen J, Prevot ASH, Worsnop DR, Baltensperger U, Coe H. A mass spectrometric study of secondary organic aerosols formed from the photooxidation of anthropogenic and biogenic precursors in a reaction chamber. *Atmos Chem Phys*, 2006, 6: 5279–5293
- 35 Gao S, Keywood M, Ng NL, Surratt J, Varutbangkul V, Bahreini R, Flagan RC, Seinfeld JH. Low-molecular-weight and oligomeric components in secondary organic aerosol from the ozonolysis of cycloalkenes and alpha-pinene. *J Phys Chem A*, 2004, 108: 10147–10164
- 36 Kostenidou E, Pathak RK, Pandis SN. An algorithm for the calculation of secondary organic aerosol density combining ams and smps data. *Aerosol Sci Technol*, 2007, 41: 1002–1010
- 37 Ng NL, Kroll JH, Chan AWH, Chhabra PS, Flagan RC, Seinfeld JH. Secondary organic aerosol formation from m-xylene, toluene, and benzene. *Atmos Chem Phys*, 2007, 7: 3909–3922
- 38 Presto AA, Hartz KEH, Donahue NM. Secondary organic aerosol production from terpene ozonolysis. 2. Effect of  $\text{NO}_x$  concentration. *Environ Sci Technol*, 2005, 39: 7046–7054
- 39 Chu B, Wang K, Takekawa H, Li J, Zhou W, Jiang J, Ma Q, He H, Hao J. Hygroscopicity of particles generated from photooxidation of  $\alpha$ -pinene under different oxidation conditions in the presence of sulfate seed aerosols. *J Environ Sci*, 2014, 26: 129–139
- 40 Varutbangkul V, Brechtel FJ, Bahreini R, Ng NL, Keywood MD, Kroll JH, Flagan RC, Seinfeld JH, Lee A, Goldstein AH. Hygroscopicity of secondary organic aerosols formed by oxidation of cycloalkenes, monoterpenes, sesquiterpenes, and related compounds. *Atmos Chem Phys*, 2006, 6: 2367–2388
- 41 Tursic J, Grgic I. Influence of  $\text{NO}_2$  on S(IV) oxidation in aqueous suspensions of aerosol particles from two different origins. *Atmos Environ*, 2001, 35: 3897–3904
- 42 Liu C, Ma Q, Liu Y, Ma J, He H. Synergistic reaction between  $\text{SO}_2$  and  $\text{NO}_2$  on mineral oxides: a potential formation pathway of sulfate aerosol. *Phys Chem Chem Phys*, 2012, 14: 1668–1676
- 43 Bai Y, Thompson GE, Martinez-Ramirez S. Effects of  $\text{NO}_2$  on oxidation mechanisms of atmospheric pollutant  $\text{SO}_2$  over baumberger sandstone. *Build Environ*, 2006, 41: 486–491
- 44 Zhang JY, Hartz KEH, Pandis SN, Donahue NM. Secondary organic aerosol formation from limonene ozonolysis: homogeneous and heterogeneous influences as a function of  $\text{NO}_x$ . *J Phys Chem A*, 2006, 110: 11053–11063
- 45 Liu C, Chu B, Liu Y, Ma Q, Ma J, He H, Li J, Hao J. Effect of mineral dust on secondary organic aerosol yield and aerosol size in  $\alpha$ -pinene/ $\text{NO}_x$  photo-oxidation. *Atmos Environ*, 2013, 77: 781–789
- 46 Zheng B, Zhang Q, Zhang Y, He KB, Wang K, Zheng GJ, Duan FK, Ma YL, Kimoto T. Heterogeneous chemistry: a mechanism missing in current models to explain secondary inorganic aerosol formation during the January 2013 haze episode in north China. *Atmos Chem Phys Discuss*, 2014, 14: 16731–16776
- 47 Na K, Song C, Switzer C, Cocker DR. Effect of ammonia on secondary organic aerosol formation from  $\alpha$ -pinene ozonolysis in dry and humid conditions. *Environ Sci Technol*, 2007, 41: 6096–6102